CHAPTER 1

Basics of Biotechnology

SUMMARY

Advances in both molecular biology and genetic engineering have enabled a modern approach to manipulating many organisms for industrial purposes. The applications of biotechnology have produced higher-yielding or pest-resistant crops; more favorable characteristics in livestock; and improved wines, cheeses, beer, and even medicines. The experiments of Gregor Mendel, the founder of modern genetics, provided the initial understanding of how traits are inherited, specifically in pea plants. After Gregor Mendel's ground-breaking work on inheritance, the structure of deoxyribonucleic acid (DNA) was determined. This eventually led to the concept of the central dogma of genetics, which states that the flow of genetic information is from DNA to proteins through an intermediate molecule called ribonucleic acid (RNA). Therefore, the flow of information resembles the following: DNA → intermediary RNA → protein. This process is universal across the three domains of life.

One of the unifying themes in life is that the genetic information is encoded in the specific sequence of nucleotides in DNA. To understand biotechnology, one must have a basic understanding of nucleic acid structure. Nucleic acids are polymers of nucleotides that are linked together by a phosphodiester bond. Each nucleotide has three basic parts: a five-carbon sugar called a pentose, a phosphate group located on the 5′ end, and a nitrogenous base. The nucleotides in DNA differ slightly from those found in RNA. In RNA, the pentose is called ribose. In DNA, it is called deoxyribose. The difference is that deoxyribose is missing a hydroxyl functional group at the 2′ position. This hydroxyl is present in ribose. The nitrogenous bases of DNA nucleotides include adenine, cytosine, guanine, and thymine; whereas in RNA, uracil replaces thymine. One last major difference between the two nucleic acids is that RNA is often found as a single strand but DNA is double-stranded—hence, the phrase *double helix*. The two strands of DNA in the double helix run in opposite directions, much like traffic on a street. On one side, the strand runs 5′ to 3′, and then returns on the opposite side with 3′ to 5′. This is termed antiparallel. The nitrogenous bases form hydrogen bonds between complementary bases in the middle of the helix: two bonds between adenine and thymine and three bonds between guanine and cytosine. When base pairing, it is always a purine (guanine and adenine) paired with a pyrimidine (cytosine, guanine, and RNA's uracil).

The three-dimensional shape of the double helix is partly dependent on the specific environmental conditions. The most common form is the B-form, in which there are about 10 bases per helix turn. Under high salt conditions, the A-form may be dominant (11 bases per turn). In some conditions, DNA could even rotate to the left and have 12 bases per turn; this is called the Z-form.

DNA contains thousands of genes and is quite long. Many proteins, some of which are enzymes, play a role in condensing and packaging DNA to fit into the tiny space of the cell. In bacteria, DNA is supercoiled into loops and then attached to a protein scaffold. In eukaryotes and many Archaea, the DNA is wrapped around histone proteins and then further condensed into fibers that are attached to a protein scaffold. The level of condensation of the DNA reflects on the level of gene expression that occurs from those regions.

Bacteria are ubiquitous, meaning that they are literally everywhere. They are extremely diverse and inhabit almost every environmental niche, ranging from frozen lakes in Antarctica, to hot springs and thermal vents on the ocean floor. Biotechnology has exploited some of the components of the diverse metabolisms of bacteria. Enzymes from a heat-loving bacterium are used in procedures such as polymerase chain reaction (PCR), in which a heat-stable enzyme is required.

Despite its usual negative publicity, *Escherichia coli* is the workhorse of molecular biology due to its relatively easy growth, maintenance, and genetic manipulation. *E. coli* often contains extra pieces of DNA called plasmids, which are used to manipulate and transfer genes between cells of the same species, and sometimes even between different species. These genes are expressed into protein in the new host cells for evaluation of the gene. *E. coli* represents

just one of the bacterial species that are considered model organisms for biotechnology purposes. There are many other model bacteria from which to choose, depending on the specific research and application.

Model eukaryotic organisms also are used in biotechnology research. Yeasts are single-celled fungi that have similar chromosomal features found in human chromosomes, such as centromeres and telomeres. Yeast also have extrachromosomal pieces of DNA that can be manipulated to contain genes from other species. The life cycle of yeast includes alternating haploid and diploid forms in which genetically identical daughter cells can be produced by budding, or new combinations of genes can be produced through sexual reproduction between two mating types of yeast.

Other model eukaryotic organisms include a small roundworm called *Caenorhabditis elegans*, which is often used to investigate genetic studies of multicellular organisms because it can reproduce asexually or sexually. The common fruit fly, *Drosophila melanogaster*, is used as a multicellular eukaryotic model because its genetics are relatively simple. Additionally, many mutants are available, and they have helped elucidate genes responsible for body patterns. Model eukaryotic organisms are not strictly limited to invertebrates. The zebrafish, *Danio rerio*, has been used extensively to study developmental genetics. Zebrafish have orthologs to many of our genes. The young are born live and develop outside their mothers. Because of these two points, zebrafish can also be used to screen drugs. Also, the mouse (*Mus musculus*) genome is incredibly similar to the human genome, in terms of gene equivalencies, and is therefore a model organism for studying human genetics. Researchers might also find it useful to study genes from cell lines. Many different cell lines exist from humans, monkeys, and insects. The advantages of using cell lines are that not only can genes be expressed or deleted, but also the cellular physiological effects of the manipulations can be monitored. Finally, plant genetics can be studied using the model flowering plant called *Arabidopsis thaliana*. The small genome, ease of growth and maintenance, and genetic characteristics common to important crop plants make this plant an ideal model organism for studying plant genetics.

No living organism is safe from viral infections. Viruses must have a host because they hijack the host cell's machinery to produce many more virus particles. Viral life cycles usually adhere to one of two mechanisms: latency (also called lysogeny in bacteria) and lytic. During latency (lysogeny), the virus inserts its genetic information directly into the host cell's genome. In the lytic cycle, the virus bursts open the host cell after replication and assembly of new virus, thus killing the host. The mechanisms of action for viruses make them excellent tools to study gene expression and also to transfer genes between strains and sometimes even species. Some human viruses might be helpful in human gene therapy because they are able to deliver genes-of-interest directly into the cells.

Other extrachromosomal gene elements are exploited by biotechnologists to manipulate the genome. They include plasmids, which often contain a few genes that confer advantageous traits to the host. These traits range from toxin production to antibiotic resistance. Transposons are also called jumping genes. These genetic elements must integrate into a host's genome in order to be replicated. Transposable elements have the potential to delete genes, duplicate genes, and even invert some genes in the host's genome, providing valuable tools for biotechnologists to manipulate the genome of target organisms.

Case Study A Single Dopamine Pathway Underlies Progressive Locomotor Deficits in a *Drosophila* Model of Parkinson Disease

Thomas Riemensperger et al. (2013). *Cell Reports* 5, 952–960.

Parkinson's disease is a neurodegenerative disease caused by the loss of midbrain dopaminergic neurons (DNs) in the substantia nigra pars compacta region of the brain. These DNs are responsible for locomotor activity. As shown previously, point mutations and duplications or triplications in the gene encoding a presynaptic protein, α-synuclein, have been implicated in the decline of locomotor activity and Parkinson's disease progression. Transgenic *Drosophila* expressing human wild-type or mutant α-synuclein were used as a model for Parkinson's disease study. Additionally, the authors of this study examined neuron clusters within the *Drosophila* brain and identified clusters of DNs that were involved in Parkinson's disease-associated decline in locomotor activity.

What type of assay was used to determine the effects of various genetic manipulations on the locomotor activity within *Drosophila*?

The startle-induced negative geotaxis (SING) assay was used to assess the locomotor activity within experimental *Drosophila*. In this assay, *Drosophila* are contained within a 25 cm vertical column and startled with a mechanical stimulus (gentle tapping). Climbing up is the normal response to this stimulus. After 1 minute of climbing, the flies at the top (above 22 cm) and the flies at the bottom (below 4 cm) are counted separately. A performance index is calculated for each experimental group.

In this paper, the authors used *Drosophila* fruit flies as a model to study Parkinson's disease, a neurodegenerative locomotor disease in humans. How is this insect model comparable to a mammalian disease?

The *Drosophila* studies in this paper indicate that in flies expressing human α-synuclein, specifically α-*synA30P* mutant, locomotor activity was impaired relative to wild-type as observed using the SING assay. Furthermore, the authors identified specific subsets of DNs located within the protocerebral anterior medial (PAM) cluster of *Drosophila* that are comparable to the midbrain DNs of the substantia nigra pars compacta in humans that are involved in Parkinson's disease.

What is the role of α-synuclein in this study?

α-Synuclein protein is a presynaptic protein within the human brain. As previously shown, overexpression of α-synuclein, either by point mutation and duplication or triplication of the gene, has been implicated in the onset of inherited forms of Parkinson's disease. Expression of this human protein within *Drosophila* brain produces a decline in locomotor activity as observed by the SING assay.

How were the authors able to locate a specific cluster of DNs within the *Drosophila* brain that was involved in the SING phenotype?

The authors evaluated SING behavior in flies that produced α-synuclein with various Gal4 drivers that are expressed within subsets of DNs. Gal4 is an expression system for *Drosophila*. The assays included Ddc-Gal4, which contained elements from Dopa decarboxylase (Ddc). The Ddc driver targets both dopaminergic and serotonergic cell clusters. These subsets were investigated using TH-Gal4 (dopaminergic) and TRH-Gal4 (serotonergic). The SING phenotype was observed in flies expressing α-synuclein with Ddc-Gal4, but not with either of the subsets (TH-Gal4 or TRH-Gal4). Out of all three of these drivers, only the Ddc-Gal4 expresses in the PAM cluster of DNs within the *Drosophila* brain. The authors further investigated the role of the PAM cluster on the SING phenotype by expressing both α-synuclein and NP6510-Gal4, which targets about 15 DNs within the PAM cluster. Similar decline in SING behavior was observed and to the same extent as the original Ddc-Gal4 expression.

Specifically, what regions of the *Drosophila* brain are involved in the SING phenotype?

The mushroom body (MB) is a structure located within the anterior hemisphere of the *Drosophila* brain. This structure is known to control locomotor activity as well as several other activities, including olfactory memorization and sleep. The authors determined that the specific region of the MB involved in locomotor control were the α′/β′ lobes, specifically the projections of NP6510 DNs into the β′ lobes. The PAM cluster contains the cell bodies for DNs that are also involved in locomotor activity. The results from this article suggest that locomotor activity is derived from both of these parts.

The loss of locomotor control during Parkinson's disease in humans results from the degeneration of DNs located within the substantia nigra pars compacta of the human brain. The authors utilized a transgenic insect model to determine the effects of human α-synuclein overexpression on locomotor activity using the SING assay. The authors determined the SING phenotype in the flies upon expression of human α-synuclein is due to the loss of function within a subset of DNs within a region of the *Drosophila* brain called the PAM cluster. The role of these PAM DNs in locomotor decline within *Drosophila* is comparable to the function of the DNs within the substantia nigra pars compacta of the human brain. Thus, the *Drosophila* model has provided researchers insight into the role of these DNs in the decline of locomotor control observed in Parkinson disease in humans.

Cell Reports
Report

A Single Dopamine Pathway Underlies Progressive Locomotor Deficits in a *Drosophila* Model of Parkinson Disease

Thomas Riemensperger,[1,2,*] Abdul-Raouf Issa,[1,4] Ulrike Pech,[2,4] Hélène Coulom,[3] Mỹ-Vân Nguyễn,[1] Marlène Cassar,[1] Mélanie Jacquet,[1] André Fiala,[2] and Serge Birman[1,3,*]

[1]Genetics and Physiopathology of Neurotransmission, Neurobiology Unit, CNRS, ESPCI ParisTech, 10 rue Vauquelin, 75005 Paris, France
[2]Molecular Neurobiology of Behaviour, Johann-Friedrich-Blumenbach Institute, Georg-August-University of Goettingen, Schwann-Schleiden Research Center, Julia-Lermontowa Weg 3, 37077 Goettingen, Germany
[3]Developmental Biology Institute of Marseille-Luminy, CNRS, Université de la Méditerranée, Campus de Luminy Case 907, 13009 Marseille, France
[4]These authors contributed equally to this work
*Correspondence: serge.birman@espci.fr (S.B.), triemen@gwdg.de (T.R.)
http://dx.doi.org/10.1016/j.celrep.2013.10.032

SUMMARY

Expression of the human Parkinson-disease-associated protein α-synuclein in all *Drosophila* neurons induces progressive locomotor deficits. Here, we identify a group of 15 dopaminergic neurons per hemisphere in the anterior medial region of the brain whose disruption correlates with climbing impairments in this model. These neurons selectively innervate the horizontal β and β′ lobes of the mushroom bodies, and their connections to the Kenyon cells are markedly reduced when they express α-synuclein. Using selective mushroom body drivers, we show that blocking or overstimulating neuronal activity in the β′ lobe, but not the β or γ lobes, significantly inhibits negative geotaxis behavior. This suggests that modulation of the mushroom body β′ lobes by this dopaminergic pathway is specifically required for an efficient control of startle-induced locomotion in flies.

INTRODUCTION

Locomotor activity in both vertebrates and invertebrates depends on signaling from the brain dopaminergic system (Beninger, 1983; Zhou and Palmiter, 1995; Giros et al., 1996; Yellman et al., 1997; Riemensperger et al., 2011). Loss of midbrain dopaminergic neurons (DNs) in the substantia nigra pars compacta in humans causes the motor symptoms of Parkinson disease (PD), the most frequent neurodegenerative movement disorder (Forno, 1996; Dauer and Przedborski, 2003; Lees et al., 2009; Shulman et al., 2011). Point mutations and duplication or triplication of the gene encoding α-synuclein (α-syn), a mainly presynaptic protein, were implicated in inherited forms of PD (Polymeropoulos, 2000; Corti et al., 2011; Devine et al., 2011). By ectopic expression of wild-type or pathogenic mutant forms of human α-syn, Feany and Bender (2000) developed the first transgenic model of PD in *Drosophila*. Flies expressing α-syn in all neurons show accelerated age-dependent locomotor deficits compared to wild-type flies, as monitored by a startle-induced negative geotaxis (SING) assay, which quantifies the climbing behavior of a fly in response to a gentle mechanical stimulus. This behavioral impairment is accompanied by a gradual loss of DNs or tyrosine hydroxylase (TH) immunoreactivity in selective cell clusters of the brain (Feany and Bender, 2000; Auluck et al., 2002, 2005; Cooper et al., 2006; Trinh et al., 2008; Barone et al., 2011; Butler et al., 2012). Furthermore, depletion of DNs using oxidative stressors such as rotenone or paraquat (Coulom and Birman, 2004; Chaudhuri et al., 2007; Hosamani et al., 2010; Lawal et al., 2010; Islam et al., 2012), as well as genetically induced dopamine (DA) deficiency in the fly brain (Riemensperger et al., 2011), severely impair SING behavior. All these results highlight the importance of brain DA for locomotor control in *Drosophila*.

Here, we use human α-syn expression to search for those specific neuronal circuits that control startle-induced locomotion in *Drosophila*. We identify a subset of 15 DNs in the protocerebral anterior medial (PAM) dopaminergic cluster whose progressive dysfunction causes deficits in SING behavior. These neurons selectively innervate the mushroom body (MB) β and β′ horizontal lobes. Consistent with this projection pattern, we find that selective blockade of neuronal activity in the MB β′ lobes impairs locomotion in the SING assay.

RESULTS AND DISCUSSION

We studied the behavioral effects of the mutant form α-synA30P, whose neuronal expression caused the strongest locomotor impairment in the *Drosophila* model of PD (Feany and Bender, 2000). In agreement with this report, we observed that *elav* > *α-synA30P* flies, in which the PD-associated protein is

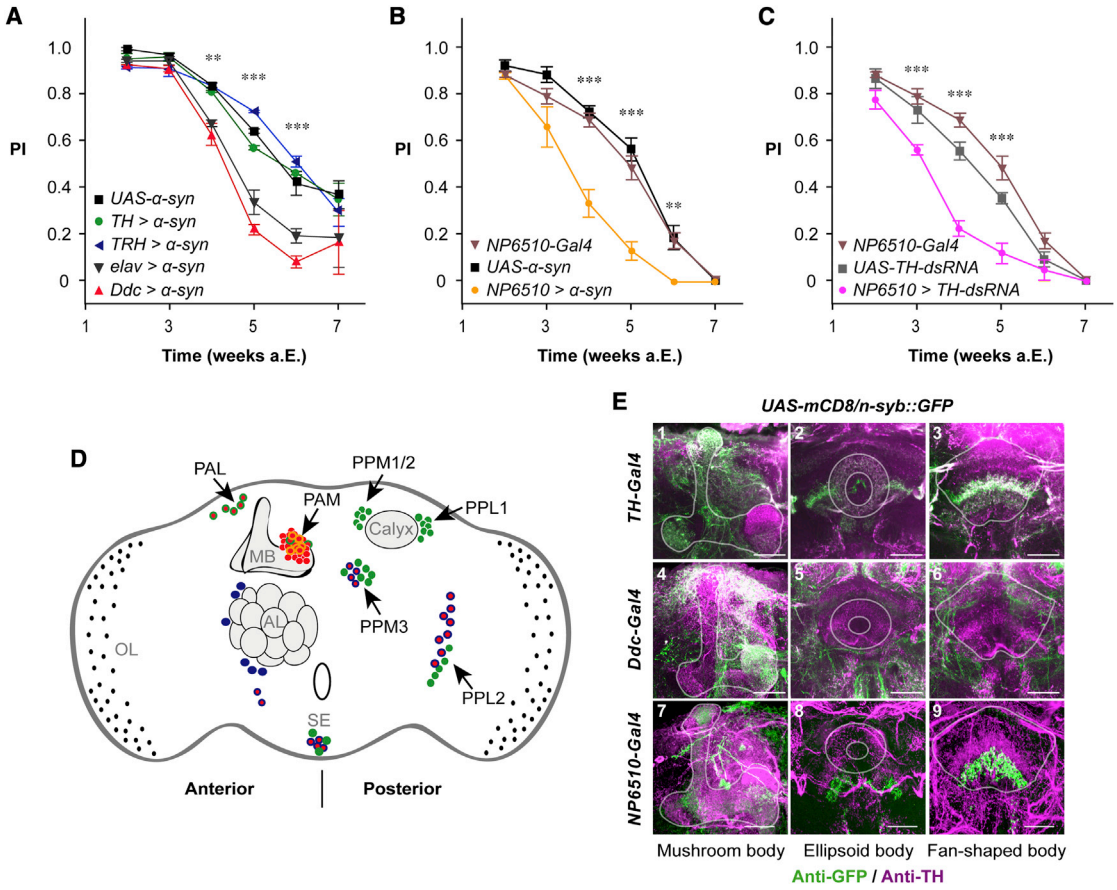

Figure 1. Expression of α-synA30P in a Single DN Cluster Evokes Locomotor Deficits

(A) Flies expressing *α-synA30P* with *elav-Gal4* (*elav* > *α-syn, gray*) or *Ddc-Gal4* (*Ddc* > *α-syn*, *red*) showed accelerated age-related locomotor (SING) decline as compared to control heterozygous *UAS-α-synA30P* flies (*UAS-α-syn*, black). In contrast, expression with *TH-Gal4* (*TH* > α-syn, green) or *TRH-Gal4* (*TRH* > *α-syn*, blue) had no significant effect.

(B) *α-synA30P* expression in a single DN cluster with *NP6510-Gal4* (*NP6510* > *α-syn*, orange) triggered SING deficits similar to *elav* > *α-syn* or *Ddc* > *α-syn* flies, compared to heterozygous *UAS-α-synA30P* (black) or *NP6510-Gal4* (brown) controls.

(C) Flies expressing a dsRNA targeting *TH* in *NP6510*-positive neurons (*NP6510* > *TH-dsRNA*, pink) showed locomotor phenotype similar to *NP6510* > *α-syn* flies. Controls were heterozygous *NP6510-Gal4* (brown) and *UAS-TH-dsRNA* (gray). **p < 0.01, ***p < 0.001; one-way ANOVA over each time point. Error bars represent SEM.

(D) Schematic depiction of the dopaminergic system and driver patterns in *Drosophila* adult brain. The driver color code corresponds to the colors of curves in (A) and (B). Left and right hemispheres represent the anterior and posterior parts of the brain, respectively. MB, mushroom bodies; AL, antennal lobes; SE, subesophagial ganglion; OL, optic lobes. Dopaminergic cluster nomenclature (Nässel and Elekes, 1992): PAL (protocerebral anterior lateral), PAM (protocerebral anterior medial), PPM (protocerebral posterior medial), PPL (protocerebral posterior lateral).

(E) Patterns of dopaminergic drivers in central brain regions revealed by expression of membrane-associated GFP. In situ coimmunostainings with anti-GFP (green) and anti-TH (magenta) antibodies. Colocalizations merge both colors in white, showing driver-targeted dopaminergic cell bodies and projections. (1–3) *TH-Gal4* drives expression in DNs projecting to the vertical lobes of the MBs and to the ellipsoid and fan-shaped bodies. (4–6) *Ddc-Gal4* strongly labels neurons projecting to the MB horizontal lobes and only weakly labels the ellipsoid and fan-shaped bodies. (7–9) *NP6510-Gal4* labels a subset of PAM DNs projecting to the horizontal lobes of the MBs, but not the ellipsoid body, whereas nondopaminergic neurons innervating the fan-shaped body are also labeled with this driver. Scale bars represent 20 μm.

See also Figures S1–S3.

expressed in all neurons, indeed show an accelerated age-dependent decline in SING performance (Figure 1A). We then compared the locomotor effects of α-syn produced with various Gal4 drivers that express in large or small subsets of DNs. Brain patterns of the different drivers used are shown in Figure S1A and schematically represented in Figure 1D. Expression using *Ddc-Gal4* or *elav-Gal4* yielded quite similar defects in this behavioral test (Figure 1A). *Ddc-Gal4* contains regulatory elements from *Dopa decarboxylase* (*Ddc*), a gene involved both in the serotonin (5-HT) and DA biosynthesis pathways (Figure S1B), and this driver accordingly targets subsets of the dopaminergic and serotonergic cell clusters (Figure S1A). Surprisingly, the expression of *α-synA30P* using the dopaminergic driver *TH-Gal4* did not induce significant impairments in this test (Figure 1A), nor did α-synA30P expression in the serotonergic system with *TRH-Gal4* induce any locomotor phenotype (Figure 1A).

Cell PRESS
Open ACCESS

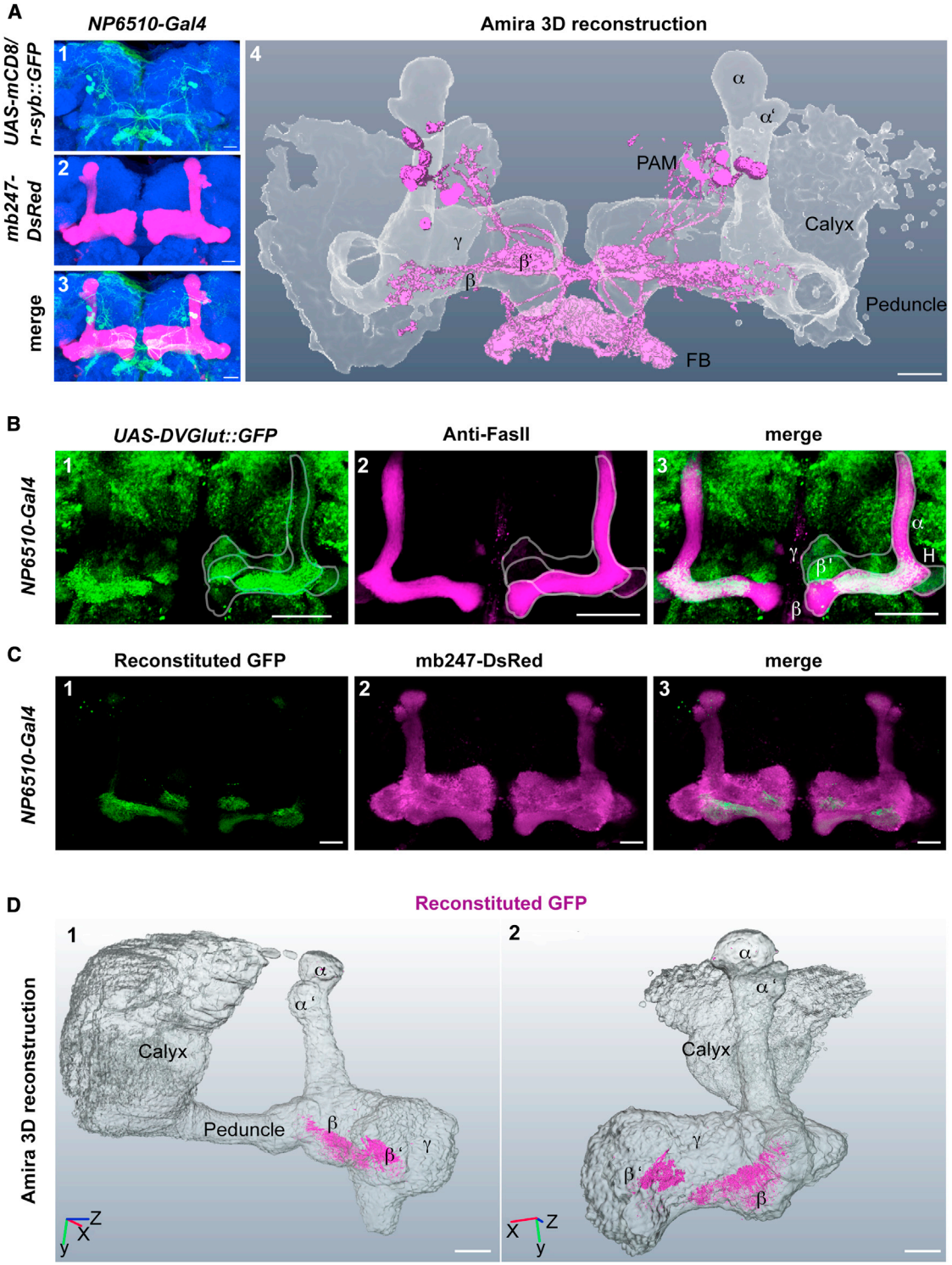

Figure 2. MB β and β′ Horizontal Lobes Receive Dopaminergic Inputs from *NP6510*-Positive PAM Neurons

(A) Whole structure of the *NP6510*-labeled PAM neurons visualized with membrane-associated GFP. (1) In situ immunostainings with anti-GFP (green), (2) MB labeling with mb247-DsRed (magenta), (3) merge, and (4) 3D Amira reconstruction. NP6510-positive DNs project from the PAM cluster into the horizontal β and β′ lobes of the MBs. Projections of nondopaminergic neurons of the same cluster pass close to the MBs and project to the fan-shaped body. Scale bars represent 20 μm.

(B) Expression of the vesicular glutamate transporter fused to GFP (DVGlut::GFP) as a synaptic vesicle marker in *NP6510* neurons. Counterstaining against MB α/β lobes with anti-Fas II antibody (2) shows that *NP6510* neurons are presynaptic to the horizontal lobes of the MBs (1), as can be seen in the merge (3).

(legend continued on next page)

TH-GAL4 strongly expresses in all brain DN clusters except the PAM cluster, which is very sparsely labeled (Friggi-Grelin et al., 2003; Mao and Davis, 2009; Pech et al., 2013a). In contrast, *Ddc-Gal4* extensively expresses in this specific cluster (Claridge-Chang et al., 2009; Liu et al., 2012; Pech et al., 2013a) (Figure S1B). We concluded that the observed negative geotaxis defects could be tentatively assigned to the PAM. This cluster consists of ~100 DNs in each hemisphere and is indeed covered by the expression pattern of *Ddc-Gal4* and *elav-Gal4* but faintly by *TH-Gal4* and not by *TRH-GAL4*. Another notable difference is that *TH-Gal4* drives expression mainly in DNs innervating the MB vertical lobes, the heel region, and the tips of the γ lobes, as well as the fan-shaped body and the ellipsoid body (Figures 1E1–1E3), whereas *Ddc-Gal4* mainly labels neurons innervating the MB horizontal lobes and only weakly the fan-shaped body and the ellipsoid body (Figures 1E4–1E6).

To assess the role of PAM neurons in SING behavior, we expressed *α-synA30P* with *NP6510-Gal4* (*NP6510*) (Liu et al., 2006; Tanaka et al., 2008; Aso et al., 2010), a driver that targets a subset of 15 DNs within the PAM cluster (Figure S2A). Strikingly, *α-synA30P* expression with *NP6510* altered SING performance to a quite similar extent as compared to pan-neuronal expression with *elav-GAL4* or *Ddc-GAL4* (Figure 1B). Expression of the wild-type form of *α-syn* in *NP6510*-positive neurons also resulted in a faster decline of SING with age (Figure S3A), but the effect was not as strong as with *α-synA30P*, as is the case with *elav-Gal4* (Feany and Bender, 2000). Furthermore, expressing a double-stranded RNA (dsRNA) to inactivate the *TH* gene selectively in *NP6510*-targeted neurons also caused an accelerated decline in SING performance, much similar to the effect of *α-synA30P* (Figure 1C). Thus, inhibiting DA synthesis in the *NP6510* DNs is sufficient to closely mimic the age-related SING defect evoked by *α-synA30P*, in agreement with the comparable SING impairment observed in brain DA-deficient flies (Riemensperger et al., 2011).

We observed that *TH*-expressing *NP6510*-positive DNs project specifically toward the tips of the β′ lobes and the middle part of the β lobes (Figure 1E7), which is comparable to the *Ddc-Gal4* MB innervation pattern (Figure 1E4). We expressed photoactivable GFP with *NP6510-Gal4* and activated the chromophore selectively in these MB regions in a single hemisphere. The diffusion of activated GFP confirmed the projection pattern of the NP6510 DNs and showed that they project to both the ipsilateral and contralateral MBs (Figures S2B1 and S2B2). Both classes of DNs appear to differ morphologically, and the DNs that innervate the β′ lobes show extensive dendritic arborizations (Figure S2B2). *NP6510* expresses in two to three other neurons whose cell bodies are located in the PAM cluster and that are not stained with an antibody against TH (Figures 1E7–1E9 and S2A), indicating that they cannot synthesize DA. These neurons, whose function is unknown, bypass the MB region and project mainly to the fan-shaped body in the contralateral hemisphere (Figures 1E9 and 2A). This projection pattern was confirmed by GFP photoactivation as well (Figure S2B3).

As further evidence of the specific role of the PAM DNs in locomotion control, we expressed *α-synA30P* with *R58E02-Gal4*, a driver that specifically labels a large part (~80%) of the PAM neurons in the central brain (Liu et al., 2012; Pech et al., 2013a). Although heterozygous *R58E02-Gal4* flies already show a faster age-related SING decline, *α-synA30P* expression with this driver significantly further impaired locomotion (Figure S3B). Interestingly, *R58E02*-positive neurons project to the horizontal lobes of the MBs, like the *NP6510* DNs, but not the ellipsoid or fan-shaped body (Figure S3C).

These results suggest that the observed locomotor phenotype could derive from altered signaling between the PAM DNs and the MB horizontal lobes. We then characterized the *NP6510*-targeted neurons further by (1) expressing in these cells the synaptic vesicle marker DvGlut::GFP to localize their presynaptic terminals (Figure 2B) and (2) using the split-GFP reconstitution across synaptic partners (GRASP) technique (Feinberg et al., 2008; Gordon and Scott, 2009; Pech et al., 2013a) to visualize direct connections of these neurons to the MBs (Figures 2C and 2D). These complementary anatomical approaches established that the *NP6510* DNs are presynaptic to the MB horizontal lobes.

By using the split-GFP reconstitution technique, we found that *α-synA30P* expression provoked an apparent decrease in *NP6510*-positive dopaminergic terminals connected to the middle part of the MB β lobes and the tip of the β′ lobes in 3-day-old adult flies, compared to control flies of the same age (Figures 3A1 and 3B1). This is attested by a volumetric analysis of the GRASP signal between *NP6510*-positive DNs and MB Kenyon cells in the horizontal lobes (Figure 3C1). In 20-day-old flies, this effect was drastic with an almost complete disappearance of dopaminergic connections, particularly in the β′ lobes (Figures 3A2–3C2). These results indicate that the synaptic terminal loss starts very early, possibly before pupal eclosion, and continues to progress significantly in the course of adult life, demonstrating that it is a degenerative process. In contrast, we did not detect overt loss of DN cell bodies in the PAM cluster and projections of nondopaminergic *NP6510* neurons toward the fan-shaped bodies were not modified by the accumulation of α-synA30P (Figure S4). This suggests that expression of pathogenic *α-synA30P* in the NP6510 DNs leads to a disruption of localized synaptic structures afferent to the MB horizontal lobes that may ultimately cause locomotion failure. Similarly, in mouse models of PD, α-syn overexpression was shown to induce degeneration of striatal terminals and locomotor deficits without obvious cell death (Scott et al., 2010; Lim et al., 2011; Lundblad et al., 2012). It can be noted that a large part of the connections between DNs and Kenyon cells are already lost when the SING performance starts to decrease (see Figure 1B). This is reminiscent of the human PD conditions in which major DN loss

(C) The two-component split-GFP system (GRASP) was employed to visualize spatial connections between *NP6510* DNs and MB Kenyon cells. CD4::spGFP1-10 was expressed in *NP6510* neurons, and CD4-Split-GFP11 and DsRed were coexpressed in α, β, and γ, as well as in α′ and β′ lobes, under control of the MB-specific promoter *mb247*. (1) Reconstituted GFP, (2) mb247-DsRed, and (3) merge.
(D) 3D Amira reconstruction of the reconstituted GFP signal. Lateral (1) and frontal (2) views. Synapses are present in the β lobes and the tip of the β′ lobes, but not in the α, α′, and γ lobes. Scale bars represent 20 μm.

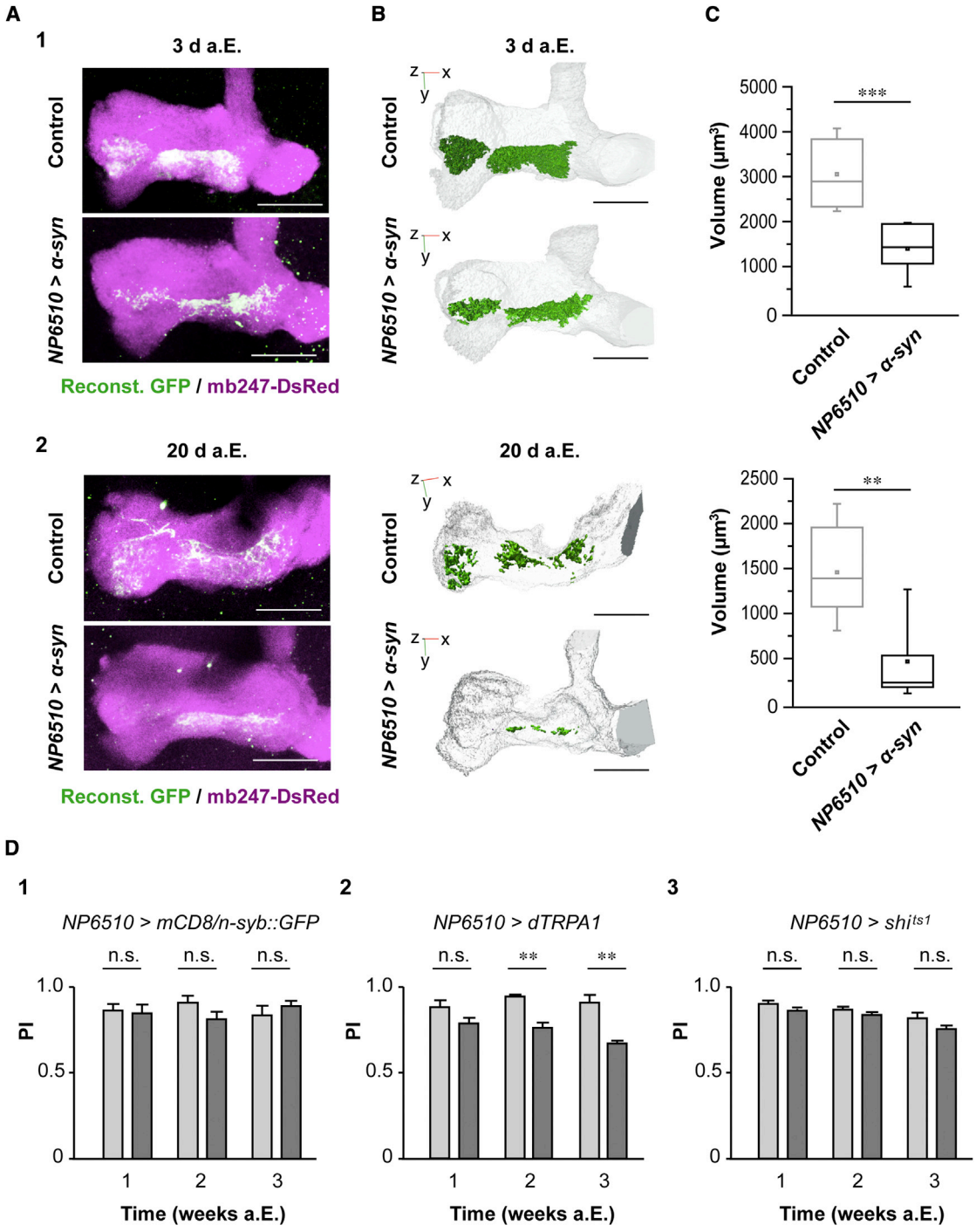

Figure 3. Reduced Connectivity between Dopaminergic PAM Neurons and MB Kenyon Cells in the Presence of α-synA30P

(A) Visualization of cell-cell contacts by split-GFP reconstitution 3 days (1) and 20 days (2) after adult eclosion in representative MBs of control animals (top panels) and flies expressing α-synA30P in NP6510 DNs (bottom panels). Merge of reconstituted Split-GFP (GRASP) signal (Reconst. GFP, green) and MB-specific expression of DsRed (mb247-DsRed, magenta) appears in white.

(B) 3D Amira reconstruction of representative MBs (gray) and their dopaminergic innervation (green). Same experimental conditions as in (A).

(C) Volumetric analysis of reconstituted split-GFP signal between *NP6510* DNs and Kenyon cells in the area of the horizontal β and β′ lobes of the MBs in the absence (control) or presence of *α-synA30P*, 3 days and 20 days after eclosion (a.E.). Box-and-whisker plots represent the median (horizontal line), the mean (square), 25% and 75% quartiles (box), and 10% and 90% quantiles (whiskers). $^{**}p < 0.01$, $^{***}p < 0.001$; one-way ANOVA.

(D) Effect of prolonged Ca^{2+} stress in *NP6510*-positive DNs. Flies expressing the heat-inducible cation channel dTRPA1 in a subset of PAM neurons show SING defects 2 and 3 weeks after eclosion when kept on elevated temperature for 12 hr each day (panel 2). Flies similarly treated that expressed either GFP as control

(legend continued on next page)

precedes the first motor symptoms of the disease. Dopaminergic connections also decreased with age in control animals, suggesting that this loss could be responsible in part for the regular SING decline in aging wild-type flies.

Subsequently, we tried to mimic the effect of transgenic expression of *α-synA30P* on startle-induced locomotion by transiently impairing activity of the *NP6510*-positive neurons by two genetic means. We either periodically silenced synaptic transmission in this subset of the PAM neurons with the temperature-sensible shi^{ts1} mutant of dynamin (Kitamoto, 2001) or stressed these neurons through repeated influx of Ca^{2+} ions with the cation-permeant thermal sensor channel dTRPA1 (Hamada et al., 2008). Adult flies expressing *GFP*, *dTRPA1*, or shi^{ts1} in NP6510 neurons were alternately incubated every day at 31°C for 12 hr and at 25°C for 12 hr, and their locomotion was tested at 7, 15, and 21 days after eclosion (Figure 3D). Compared to *NP6510 > GFP* flies as a control (Figure 3D1), sustained dTRPA1 activation progressively decreased SING performance (Figure 3D2), as is the case with flies expressing *α-synA30P* or a dsRNA against *TH* in the same neurons (Figures 1B and 1C). In contrast, periodical inhibition of synaptic transmission with shi^{ts1} did not impair negative geotaxis (Figure 3D3). This suggests that sustained influx of cations mediated by dTRPA1 for 12 hr a day progressively altered neuronal functioning, thus mimicking the deleterious effects of α-synA30P, whereas silencing synaptic activity with shi^{ts1} for long periods of time had no comparable negative effect.

The MB is a paired brain structure involved in several essential brain functions, like olfactory memory formation (Heisenberg, 2003; Fiala, 2007; Davis, 2011; Kahsai and Zars, 2011; Waddell, 2013), sleep (Bushey and Cirelli, 2011) and the control of locomotor activity (Howse, 1975; Martin et al., 1998; Helfrich-Förster et al., 2002; Serway et al., 2009). Here, we tried to identify regions of the MBs involved in locomotion control. For that purpose, we either silenced or overstimulated the different MB lobes by incubating at 31°C for 10 min flies that expressed shi^{ts1} or *dTRPA1*, respectively, with MB specific drivers, before subjecting these flies to the SING paradigm. We used *c305a-Gal4* to target selective expression in the α′/β′ and faintly γ lobes, but not in the α/β lobes (Krashes et al., 2007; Pech et al., 2013b), and *mb247-Gal4* that expresses in α/β and γ lobes, but not in α′/β′ lobes (Zars et al., 2000; Krashes et al., 2007; Pech et al., 2013a, 2013b) (Figure 4A). With these drivers, we found that either silencing or overstimulation of the α′/β′ lobes, but not of the other MB lobes, had similar strong inhibitory effects on climbing activity of the flies (Figures 4B and 4C). These results substantiate the conclusion that projections of the *NP6510* DNs to the β′ lobes can potently modulate a startle-induced locomotor response.

The PAM cluster comprises different subtypes of DNs implicated in distinct behaviors, notably in aversive and appetitive reinforcement of olfactory memory (Waddell, 2013). Interestingly, it was reported that the *NP6510* DNs are not involved in associative learning and memory (Aso et al., 2010). This suggests that these neurons and the specific Kenyon cells they innervate could be specifically involved in locomotion control. Thereby, the insect dopaminergic system shares a similarity with that of vertebrates, whose DNs are most prominently implicated in either learning and memory or locomotion control (Dunnett et al., 2005).

In conclusion, our results demonstrate that the SING phenotype in the Feany and Bender PD model primarily derives from gradual dysfunction of a subset of DNs in the PAM cluster without overt cell death. Progressive disruption of synaptic structure or activity in these cells by sustained *α-synA30P* or *TH-dsRNA* expression, or by dTRPA1 activation, all impaired the fly's climbing ability. Strikingly, the expression of *α-synA30P* in these 2 × 15 DNs progressively altered locomotion to the same extent as the expression of the pathogenic protein in the ~100,000 neurons of the *Drosophila* brain. These PAM DNs and the MB β′ lobe Kenyon cells they innervate form a neuronal circuit involved in control of SING behavior. These DNs are very susceptible to α-syn toxicity and they play an important role in locomotion, comparably to the midbrain DNs in humans whose degeneration causes the motor symptoms of PD. Thus, in flies, as in humans, motor impairments in PD conditions correlate to the degeneration of a specific subset of brain DNs located in the substantia nigra pars compacta in humans and in the PAM cluster in *Drosophila*. This opens the way for future studies in a genetically tractable organism to decipher the pathological pathways activated by α-syn that cause disruption of these dopaminergic projections as well as the cellular interaction mechanisms leading from dopaminergic terminal loss to progressive locomotor dysfunction.

EXPERIMENTAL PROCEDURES

Drosophila Culture and Strains

Fly stocks and crosses were raised at 25°C on standard corn meal/yeast/agar medium supplemented with methyl-4-hydroxy-benzoate as a mold protector, under a 12 h/12 hr light/dark cycle. The following fly strains were from the Bloomington Drosophila Stock Center: *elav-GAL4* ($elav^{C155}$, #458), *UAS-TH-dsRNA* (*TriP JF01813,* #25796); *UAS-mCD8::GFP* (#5137), *UAS-n-syb::GFP* (#6921). An *UAS-mCD8::GFP*, *UAS-n-syb::GFP* strain (here named *UAS-mCD8/n-syb::GFP*) was obtained by meiotic recombination and used to visualize whole neuronal structures. Other strains were *Ddc-Gal4 (HL8.6)* (Li et al., 2000), *TH-Gal4* (Friggi-Grelin et al., 2003), *TRH-Gal4* (Pech et al., 2013a), *NP6510-Gal4* (Liu et al., 2006), *R58E02-Gal4* (Liu et al., 2012), *c305a-Gal4* (Krashes et al., 2007), *mb247-Gal4* (Zars et al., 2000), *mb247-DsRed* (Riemensperger et al., 2005; Pech et al., 2013b), *UAS-α-synWT* and *UAS-α-synA30P* (Feany and Bender, 2000), *UAS-C3PA-GFP* (Ruta et al., 2010), *UAS-DVGlut::GFP* (T. Rival and S.B., unpublished data), *UAS-*shi^{ts1} (Kitamoto, 2001), and *UAS-dTRPA1* (Hamada et al., 2008).

Negative Geotaxis

SING was assayed as previously described (Coulom and Birman, 2004; Rival et al., 2004). Groups of 10 to 20 flies were placed in a vertical column (25 cm long, 1.5 cm diameter) with a conic bottom end. They were suddenly startled by gently tapping them down, to which *Drosophila* respond by climbing up.

(panel 1) or shi^{ts1} that inhibits neurotransmitter release above 30°C (panel 3) do not show significant decline in their locomotor performance. Light gray bars: adult flies continuously at 25°C. Dark gray bars: adult flies alternately incubated 12 hr at 31°C and 12 hr at 25°C. **$p < 0.01$; Mann-Whitney U test. Error bars represent SEM.
See also Figure S4.

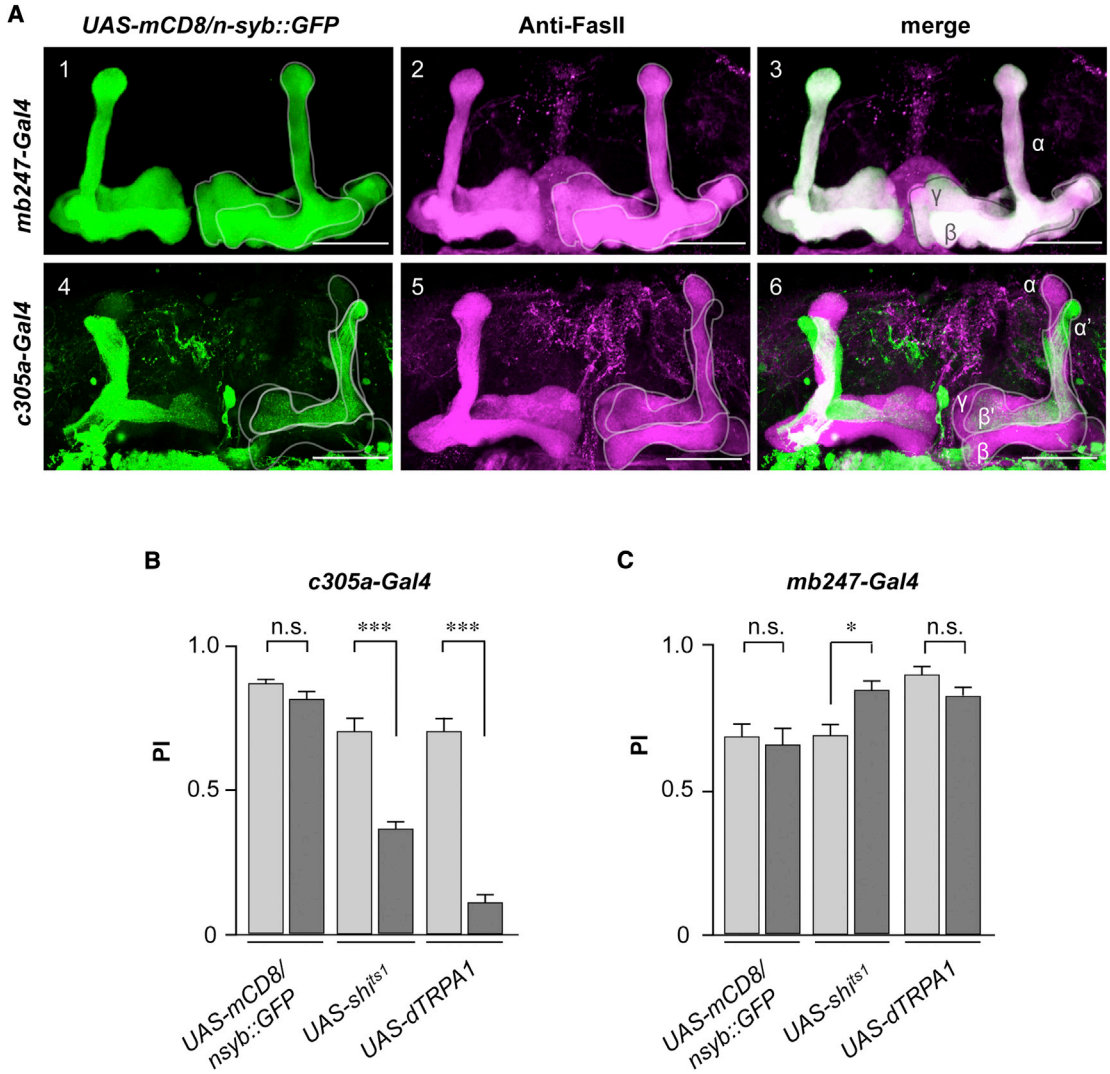

Figure 4. Activity of the MB Prime Lobes Controls Startle-Induced Locomotion

(A) Expression patterns of mushroom body drivers. *mb247-Gal4* (1–3) shows staining in α/β and γ lobes, but not in α′/β′. In contrast, *c305a-Gal4* (4–6) primarily expresses in α′/β′ lobes. Immunostaining against GFP (green) and counterstaining with anti-FasII (magenta) that only labels the α/β and γ lobes. Colocalizations appear in white. Scale bars represent 50 μm.

(B) Perturbations of MB β′ lobe signaling interfere with the SING response. Expression of either *shi*^{ts1} or *dTRPA1* with the α′/β′ driver *c305a-Gal4* decreased negative geotaxis performance after 10 min incubation at elevated temperature (31°C, dark gray bars), compared to unheated controls (23°C, light gray bars). Flies were aged 7–10 days a.E. ***p < 0.001, Mann-Whitney U test.

(C) Artificial activation of α/β and γ lobes with *mb247-Gal4* triggered no decrease in locomotor performance (p = 0.1431). Silencing with *shi*^{ts1} showed a slightly positive effect (p = 0.029). Same procedures as in (B). Error bars represent SEM.

After 1 min, flies having reached the top of the column (above 22 cm) and flies remaining at the bottom end (below 4 cm) were separately counted. Three rounds per column were performed at 1 min intervals. Results are the mean ± SEM of the scores obtained with five to 15 independent groups of flies per genotype. The performance index (PI) is defined as $\frac{1}{2}[(n_{tot} + n_{top} - n_{bot})/n_{tot}]$, where n_{tot}, n_{top}, and n_{bot} are the total number of flies, the number of flies at the top, and the number of flies at the bottom, respectively. To test for the effect of aging, flies of each condition were evaluated each week throughout a period of 7 weeks. Dead flies were replaced by substitutes of the same age. The same experiments were repeated two or three times at different periods of the year. For silencing or overstimulation of MB neurons, 7- to 10-day-old flies expressing *shi*^{ts1} or *dTRPA1*, respectively, were incubated for 10 min at 31°C, or at 23°C for controls, just before the SING assay. Statistical analyses were performed with GraphPad Prism (GraphPad Software) using Mann-Whitney U test or one-way ANOVA with the post hoc Tukey-Kramer test. Error bars in figures represent SEM.

Immunohistochemistry

Adult brains were dissected in ice-cold *Drosophila* Ringer's solution and processed for whole-mount immunostaining as previously described (Riemensperger et al., 2011). The following primary antibodies were used: mouse monoclonal anti-TH (ImmunoStar, 1:50), rabbit anti-GFP (Invitrogen Molecular Probes, 1:500), mouse monoclonal anti-Fasciclin II (FasII) (Developmental Studies Hybridoma Bank, 1:50). The secondary antibodies were goat anti-mouse

or anti-rabbit conjugated to Alexa Fluor 488 or 555 (Invitrogen Molecular Probes, 1:500). Images were acquired with a Nikon A1R confocal microscope.

GFP Photoactivation

Brains of 7-day-old *mb247-DsRed; NP6510-Gal4/UAS-C3PA-GFP* female flies were dissected in ice-cold Ringer's solution. The regions of interests within the MBs, spotted by mb247-DsRed fluorescence, were selectively scanned in their three dimensions at 760 nm with 5% laser power and 0.53 μs pixel dwell time using a Zeiss LSM7 MP two-photon microscope equipped with a Zeiss w-Plan Apochromat 20× water immersion objective (NA = 1.0). Each pixel was excited 25 times in intervals of ~1 min each. The activated PA-GFP molecules were allowed to diffuse for 45 min before the brains were scanned again at 950 nm excitation and PA-GFP and dsRed fluorescence were recorded simultaneously using a dichroic mirror in combination with 500–550 nm and 575–610 nm emission filters.

Split-GFP Reconstitution across Synaptic Partners

For the visualization of connectivity between DNs and Kenyon cells with the GRASP method (Feinberg et al., 2008; Gordon and Scott, 2009), the strain *mb247-DsRed*; *mb247-CD4::spGFP11*, *UAS-CD4::spGFP1-10* (Pech et al., 2013a) was crossed to *NP6510-Gal4*, and observations were carried out on 5- to 6-day-old progeny females (raised at 25°C and 60% humidity). Brains were dissected and mounted in Ringer's solution, with the anterior side facing upward. Image stacks covering 180 μm were acquired at 0.6 μm z steps using a Zeiss LSM7 MP two-photon microscope, equipped with a w-plan apochromat 20× water immersion objective, an excitation of 8% laser power at 950 nm, a pixel dwell of 2.3 μs, an x/y resolution of 0.18 μm/pixel, and a line average of 4. GRASP fluorescence and dsRed fluorescence were recorded simultaneously, using a dichroic mirror in combination with 500–550 nm and 575–610 nm emission filters. To compensate for changes in detected intensity due to the depth of the optical slice within the brain, gain was adjusted manually (8% decrease from deepest to most anterior slice).

To analyze the effect of α-synA30P on connectivity, we generated mb247-DsRed/UAS-α-synA30P; NP6510-Gal4/mb247-CD4::spGFP11, UAS-CD4::spGFP1-10 flies and compared them to mb247-DsRed/CyO; NP6510-Gal4/mb247-CD4::spGFP11, UAS-CD4::spGFP1-10 sib progeny as control 3 and 20 days after eclosion. Brains of those flies were immunostained as described above, using the anti-GFP20 primary antibody (Sigma-Aldrich G6539, 1:200) that specifically recognizes reconstituted split-GFP (Gordon and Scott, 2009; Pech et al., 2013a). Immunostainings were performed in parallel for all brains, using a mastermix of reagents, and all image stacks were captured on the same day, using exactly equal microscope settings. Images were processed using the Fiji Software (Schindelin et al., 2012). For reconstruction, Amira 5.3.3 software (Visage Imaging) was used, in particular the function "label field" on either the dsRed channel or the GFP channel of the stack. Based on empiric evaluation of noise and background in control images and based on the respective background noise of each image, an intensity threshold was manually defined. For each channel, pixels above this threshold were labeled and a volumetric surface was generated (smoothed for MB label field, unsmoothed for GRASP label field). The α-synA30P-induced loss of dopaminergic terminals in the horizontal lobes was observed in three independent experiments, and volumetric analysis of reconstituted split-GFP signal was performed on ten MBs from five flies per condition. The Kolmogorov-Smirnov method was used to confirm normal distribution of the data. Statistical analysis was performed using a one-way ANOVA with the post hoc Tukey-Kramer test.

SUPPLEMENTAL INFORMATION

Supplemental Information includes four figures and can be found with this article online at http://dx.doi.org/10.1016/j.celrep.2013.10.032.

ACKNOWLEDGMENTS

We thank Dr. Mel Feany, Dr. Hiromu Tanimoto, and the TRiP at Harvard Medical School (NIH/NIGMS R01-GM084947) for providing fly stocks used in this study. This work was supported by research grants from the Agence Nationale de la Recherche (ANR-07-NEURO-028), the Fédération pour la Recherche sur le Cerveau (2008 ROTARY 4), and the Fondation de France (2009-006201) (to S.B.). The work was furthermore supported by research grants from the Deutsche Forschungsgemeinschaft (FI 821/3-1, SFB 889/B4, and SPP 1392 FI 821/2-1) and the Bundesministerium für Bildung und Forschung via the Bernstein Center for Computational Neuroscience (01GQ1005A, TP C02) (to A.F.). T.R. was the recipient of a postdoctoral fellowship from the Neuropôle de Recherche Francilien, and H.C. and M.C. received PhD contracts with the Université de la Méditerranée and Université Pierre-et-Marie-Curie, respectively.

Received: December 29, 2012
Revised: September 18, 2013
Accepted: October 21, 2013
Published: November 14, 2013

REFERENCES

Aso, Y., Siwanowicz, I., Bräcker, L., Ito, K., Kitamoto, T., and Tanimoto, H. (2010). Specific dopaminergic neurons for the formation of labile aversive memory. Curr. Biol. *20*, 1445–1451.

Auluck, P.K., Chan, H.Y.E., Trojanowski, J.Q., Lee, V.M.Y., and Bonini, N.M. (2002). Chaperone suppression of alpha-synuclein toxicity in a *Drosophila* model for Parkinson's disease. Science *295*, 865–868.

Auluck, P.K., Meulener, M.C., and Bonini, N.M. (2005). Mechanisms of Suppression of {alpha}-Synuclein Neurotoxicity by Geldanamycin in Drosophila. J. Biol. Chem. *280*, 2873–2878.

Barone, M.C., Sykiotis, G.P., and Bohmann, D. (2011). Genetic activation of Nrf2 signaling is sufficient to ameliorate neurodegenerative phenotypes in a *Drosophila* model of Parkinson's disease. Dis. Model. Mech. *4*, 701–707.

Beninger, R.J. (1983). The role of dopamine in locomotor activity and learning. Brain Res. *287*, 173–196.

Bushey, D., and Cirelli, C. (2011). From genetics to structure to function: exploring sleep in *Drosophila*. Int. Rev. Neurobiol. *99*, 213–244.

Butler, E.K., Voigt, A., Lutz, A.K., Toegel, J.P., Gerhardt, E., Karsten, P., Falkenburger, B., Reinartz, A., Winklhofer, K.F., and Schulz, J.B. (2012). The mitochondrial chaperone protein TRAP1 mitigates α-Synuclein toxicity. PLoS Genet. *8*, e1002488.

Chaudhuri, A., Bowling, K., Funderburk, C., Lawal, H., Inamdar, A., Wang, Z., and O'Donnell, J.M. (2007). Interaction of genetic and environmental factors in a *Drosophila* parkinsonism model. J. Neurosci. *27*, 2457–2467.

Claridge-Chang, A., Roorda, R.D., Vrontou, E., Sjulson, L., Li, H., Hirsh, J., and Miesenböck, G. (2009). Writing memories with light-addressable reinforcement circuitry. Cell *139*, 405–415.

Cooper, A.A., Gitler, A.D., Cashikar, A., Haynes, C.M., Hill, K.J., Bhullar, B., Liu, K., Xu, K., Strathearn, K.E., Liu, F., et al. (2006). Alpha-synuclein blocks ER-Golgi traffic and Rab1 rescues neuron loss in Parkinson's models. Science *313*, 324–328.

Corti, O., Lesage, S., and Brice, A. (2011). What genetics tells us about the causes and mechanisms of Parkinson's disease. Physiol. Rev. *91*, 1161–1218.

Coulom, H., and Birman, S. (2004). Chronic exposure to rotenone models sporadic Parkinson's disease in *Drosophila melanogaster*. J. Neurosci. *24*, 10993–10998.

Dauer, W., and Przedborski, S. (2003). Parkinson's disease: mechanisms and models. Neuron *39*, 889–909.

Davis, R.L. (2011). Traces of *Drosophila* memory. Neuron *70*, 8–19.

Devine, M.J., Gwinn, K., Singleton, A., and Hardy, J. (2011). Parkinson's disease and α-synuclein expression. Mov. Disord. *26*, 2160–2168.

Dunnett, S.B., Bentivoglio, M., Bjorklund, A., and Hökfelt, T. (2005). Dopamine, Volume 21 (Handbook of Chemical Neuroanatomy) (Elsevier Science).

Feany, M.B., and Bender, W.W. (2000). A *Drosophila* model of Parkinson's disease. Nature *404*, 394–398.

Feinberg, E.H., Vanhoven, M.K., Bendesky, A., Wang, G., Fetter, R.D., Shen, K., and Bargmann, C.I. (2008). GFP Reconstitution Across Synaptic Partners (GRASP) defines cell contacts and synapses in living nervous systems. Neuron *57*, 353–363.

Fiala, A. (2007). Olfaction and olfactory learning in *Drosophila*: recent progress. Curr. Opin. Neurobiol. *17*, 720–726.

Forno, L.S. (1996). Neuropathology of Parkinson's disease. J. Neuropathol. Exp. Neurol. *55*, 259–272.

Friggi-Grelin, F., Coulom, H., Meller, M., Gomez, D., Hirsh, J., and Birman, S. (2003). Targeted gene expression in *Drosophila* dopaminergic cells using regulatory sequences from tyrosine hydroxylase. J. Neurobiol. *54*, 618–627.

Giros, B., Jaber, M., Jones, S.R., Wightman, R.M., and Caron, M.G. (1996). Hyperlocomotion and indifference to cocaine and amphetamine in mice lacking the dopamine transporter. Nature *379*, 606–612.

Gordon, M.D., and Scott, K. (2009). Motor control in a *Drosophila* taste circuit. Neuron *61*, 373–384.

Hamada, F.N., Rosenzweig, M., Kang, K., Pulver, S.R., Ghezzi, A., Jegla, T.J., and Garrity, P.A. (2008). An internal thermal sensor controlling temperature preference in *Drosophila*. Nature *454*, 217–220.

Heisenberg, M. (2003). Mushroom body memoir: from maps to models. Nat. Rev. Neurosci. *4*, 266–275.

Helfrich-Förster, C., Wulf, J., and de Belle, J.S. (2002). Mushroom body influence on locomotor activity and circadian rhythms in *Drosophila melanogaster*. J. Neurogenet. *16*, 73–109.

Hosamani, R., Ramesh, S.R., and Muralidhara. (2010). Attenuation of rotenone-induced mitochondrial oxidative damage and neurotoxicty in *Drosophila melanogaster* supplemented with creatine. Neurochem. Res. *35*, 1402–1412.

Howse, P.E. (1975). Brain structure and behavior in insects. Annu. Rev. Entomol. *20*, 359–379.

Islam, R., Yang, L., Sah, M., Kannan, K., Anamani, D., Vijayan, C., Kwok, J., Cantino, M.E., Beal, M.F., and Fridell, Y.-W.C. (2012). A neuroprotective role of the human uncoupling protein 2 (hUCP2) in a *Drosophila* Parkinson's disease model. Neurobiol. Dis. *46*, 137–146.

Kahsai, L., and Zars, T. (2011). Learning and memory in *Drosophila*: behavior, genetics, and neural systems. Int. Rev. Neurobiol. *99*, 139–167.

Kitamoto, T. (2001). Conditional modification of behavior in *Drosophila* by targeted expression of a temperature-sensitive shibire allele in defined neurons. J. Neurobiol. *47*, 81–92.

Krashes, M.J., Keene, A.C., Leung, B., Armstrong, J.D., and Waddell, S. (2007). Sequential use of mushroom body neuron subsets during *drosophila* odor memory processing. Neuron *53*, 103–115.

Lawal, H.O., Chang, H.-Y., Terrell, A.N., Brooks, E.S., Pulido, D., Simon, A.F., and Krantz, D.E. (2010). The *Drosophila* vesicular monoamine transporter reduces pesticide-induced loss of dopaminergic neurons. Neurobiol. Dis. *40*, 102–112.

Lees, A.J., Hardy, J., and Revesz, T. (2009). Parkinson's disease. Lancet *373*, 2055–2066.

Li, H., Chaney, S., Roberts, I.J., Forte, M., and Hirsh, J. (2000). Ectopic G-protein expression in dopamine and serotonin neurons blocks cocaine sensitization in *Drosophila melanogaster*. Curr. Biol. *10*, 211–214.

Lim, Y., Kehm, V.M., Lee, E.B., Soper, J.H., Li, C., Trojanowski, J.Q., and Lee, V.M.-Y. (2011). α-Syn suppression reverses synaptic and memory defects in a mouse model of dementia with Lewy bodies. J. Neurosci. *31*, 10076–10087.

Liu, G., Seiler, H., Wen, A., Zars, T., Ito, K., Wolf, R., Heisenberg, M., and Liu, L. (2006). Distinct memory traces for two visual features in the *Drosophila* brain. Nature *439*, 551–556.

Liu, C., Plaçais, P.-Y., Yamagata, N., Pfeiffer, B.D., Aso, Y., Friedrich, A.B., Siwanowicz, I., Rubin, G.M., Preat, T., and Tanimoto, H. (2012). A subset of dopamine neurons signals reward for odour memory in *Drosophila*. Nature *488*, 512–516.

Lundblad, M., Decressac, M., Mattsson, B., and Björklund, A. (2012). Impaired neurotransmission caused by overexpression of α-synuclein in nigral dopamine neurons. Proc. Natl. Acad. Sci. USA *109*, 3213–3219.

Mao, Z., and Davis, R.L. (2009). Eight different types of dopaminergic neurons innervate the *Drosophila* mushroom body neuropil: anatomical and physiological heterogeneity. Front Neural Circuits *3*, 5.

Martin, J.R., Ernst, R., and Heisenberg, M. (1998). Mushroom bodies suppress locomotor activity in *Drosophila melanogaster*. Learn. Mem. *5*, 179–191.

Nässel, D.R., and Elekes, K. (1992). Aminergic neurons in the brain of blowflies and *Drosophila*: dopamine- and tyrosine hydroxylase-immunoreactive neurons and their relationship with putative histaminergic neurons. Cell Tissue Res. *267*, 147–167.

Pech, U., Pooryasin, A., Birman, S., and Fiala, A. (2013a). Localization of the contacts between Kenyon cells and aminergic neurons in the *Drosophila melanogaster* brain using splitGFP reconstitution. J. Comp. Neurol. *521*, 3992–4026.

Pech, U., Dipt, S., Barth, J., Singh, P., Jauch, M., Thum, A.S., Fiala, A., and Riemensperger, T. (2013b). Mushroom body miscellanea: transgenic *Drosophila* strains expressing anatomical and physiological sensor proteins in Kenyon cells. Front Neural Circuits *7*, 147.

Polymeropoulos, M.H. (2000). Genetics of Parkinson's disease. Ann. N Y Acad. Sci. *920*, 28–32.

Riemensperger, T., Völler, T., Stock, P., Buchner, E., and Fiala, A. (2005). Punishment prediction by dopaminergic neurons in *Drosophila*. Curr. Biol. *15*, 1953–1960.

Riemensperger, T., Isabel, G., Coulom, H., Neuser, K., Seugnet, L., Kume, K., Iché-Torres, M., Cassar, M., Strauss, R., Preat, T., et al. (2011). Behavioral consequences of dopamine deficiency in the *Drosophila* central nervous system. Proc. Natl. Acad. Sci. USA *108*, 834–839.

Rival, T., Soustelle, L., Strambi, C., Besson, M.-T., Iché, M., and Birman, S. (2004). Decreasing glutamate buffering capacity triggers oxidative stress and neuropil degeneration in the *Drosophila* brain. Curr. Biol. *14*, 599–605.

Ruta, V., Datta, S.R., Vasconcelos, M.L., Freeland, J., Looger, L.L., and Axel, R. (2010). A dimorphic pheromone circuit in *Drosophila* from sensory input to descending output. Nature *468*, 686–690.

Schindelin, J., Arganda-Carreras, I., Frise, E., Kaynig, V., Longair, M., Pietzsch, T., Preibisch, S., Rueden, C., Saalfeld, S., Schmid, B., et al. (2012). Fiji: an open-source platform for biological-image analysis. Nat. Methods *9*, 676–682.

Scott, D.A., Tabarean, I., Tang, Y., Cartier, A., Masliah, E., and Roy, S. (2010). A pathologic cascade leading to synaptic dysfunction in alpha-synuclein-induced neurodegeneration. J. Neurosci. *30*, 8083–8095.

Serway, C.N., Kaufman, R.R., Strauss, R., and de Belle, J.S. (2009). Mushroom bodies enhance initial motor activity in *Drosophila*. J. Neurogenet. *23*, 173–184.

Shulman, J.M., De Jager, P.L., and Feany, M.B. (2011). Parkinson's disease: genetics and pathogenesis. Annu. Rev. Pathol. *6*, 193–222.

Tanaka, N.K., Tanimoto, H., and Ito, K. (2008). Neuronal assemblies of the *Drosophila* mushroom body. J. Comp. Neurol. *508*, 711–755.

Trinh, K., Moore, K., Wes, P.D., Muchowski, P.J., Dey, J., Andrews, L., and Pallanck, L.J. (2008). Induction of the phase II detoxification pathway suppresses neuron loss in *Drosophila* models of Parkinson's disease. J. Neurosci. *28*, 465–472.

Waddell, S. (2013). Reinforcement signalling in *Drosophila*; dopamine does it all after all. Curr. Opin. Neurobiol. *23*, 324–329.

Yellman, C., Tao, H., He, B., and Hirsh, J. (1997). Conserved and sexually dimorphic behavioral responses to biogenic amines in decapitated *Drosophila*. Proc. Natl. Acad. Sci. USA *94*, 4131–4136.

Zars, T., Fischer, M., Schulz, R., and Heisenberg, M. (2000). Localization of a short-term memory in *Drosophila*. Science *288*, 672–675.

Zhou, Q.Y., and Palmiter, R.D. (1995). Dopamine-deficient mice are severely hypoactive, adipsic, and aphagic. Cell *83*, 1197–1209.